ELSEVIER

Journal of Chromatography A, 898 (2000) 141–151

JOURNAL OF CHROMATOGRAPHY A

www.elsevier.com/locate/chroma

Retention properties of the fluorinated bonded phase on liquid chromatography of aromatic hydrocarbons

Fumiko M. Yamamoto*, Souji Rokushika

Division of Chemistry, Graduate School of Science, Kyoto University, Sakyo-ku, Kyoto 606-8502, Japan

Received 14 March 2000; received in revised form 7 August 2000; accepted 14 August 2000

Abstract

The unique characteristics of a bonded-fluoroalkylsilane column, Fluofix, are described by comparison with those of a bonded octylsilane column, C_8, in the reversed-phase chromatography of aromatic hydrocarbons. The selectivity of homologous aromatics on the fluorinated column varied with the methanol concentration in the eluent. At a larger proportion of methanol than 80:20 (v/v) the larger aromatics eluted faster than the smaller ones. However, with less methanol, the aromatics were eluted in order of their molecular size, as usually reported for a conventional hydrocarbonaceous column. A dependence of the retention mechanism on the composition of the eluent was suggested by the decrease in the entropy–enthalpy compensation temperature, β, with increase of methanol concentration in the eluent. In order to explain the concentration dependence of the retention, the molecular interaction energy in the retention process was calculated by computer simulation. The interaction energy between aromatics and the stationary ligand on the Fluofix column was smaller than that on the C_8 column and comparable to the interaction energy between the aromatics and methanol. At higher methanol concentrations, solute–fluorinated ligand complex formation was obstructed by the methanol molecules solvating the solute, reducing the retention of the larger aromatics.

Keywords: Retention properties; Fluorinated bonded phases; Fluofix; Aromatic hydrocarbons

1. Introduction

Various fluorinated packing materials have been prepared as nonpolar materials in addition to hydrocarbonaceous materials for reversed-phase liquid chromatography (RPLC). The low polarity of the fluorinated ligand was expected to have the advantage of wide selectivity [1]. In general, the retention of solute was less on the fluorinated phases than on the corresponding hydrocarbonaceous phases [2–7]. The weak retention on the fluorinated phase is regarded as suitable for the separation of proteins with a low organic modifier in the mobile phase. Geng et al. applied a fluorinated column to the RPLC of proteins eluting with isopropanol–buffer and obtained excellent recovery of the protein [3]. The fluorinated phase retained longer the solute containing more fluorine atoms in the molecule [4,7]. The selectivity for fluorine-containing compounds is useful for separation in fields such as pharmacology and agriculture. Fluorinated adrenocortico steroids and fluorinated anti-cancer agents have been separated from their hydrocarbon analogues on a fluorocarbon column [8].

The shape recognition of the stationary phase has been studied using aromatic hydrocarbons as probes.

*Corresponding author.

0021-9673/00/$ – see front matter
PII: S0021-9673(00)00866-9

Wise and co-workers described the selectivity characteristics of monomeric and polymeric hydrocarbonaceous phases on the retention of polycyclic aromatic hydrocarbons [9–12]. The retention properties have been elucidated for various chemically bonded stationary phases, such as the triphenyl or naphthyl ethyl bonding C_{18} phase [13], the cholesteryl-silica phase [14], and the cyclophane-bonded phase [15]. The roles of the silica phase [16] and the amino-bonded silica phase [17] have been discussed for the retention of aromatics on elution with nonpolar solvents. On these columns, aromatics in a homologous series were eluted in order of increasing molecular size, and the number of π-electrons in the aromatic rings. The retention behavior has been explained in terms of the planarity of the solutes and the orderliness of the stationary ligand.

Retention of the solute has been described using retention models, such as the inserted model [18], the slot model [19], and the interphase model [20]. In these models, a solute molecule is inserted into the grafted layer in the stationary phase and retained by the formation of a complex with the ligand constituting the layer. The importance of the orientation of the solute molecule with respect to the ligand and the effects of the surrounding solvent molecules has been considered in complex formation.

The use of a computer aided the calculations using the above models. Yarovsky et al. studied the molecular modeling of the stationary ligand using a computer simulation [21]. Calculation of the quadrupole moment of polycyclic aromatics was carried out as an approach to the estimation of molecular interactions in the retention process [22]. The effects of solvent molecules on solvation have been studied by simulation using models. These are, for example, the conduct-like screening model (COSMO) method [23] and the search for the lowest-energy conformation of the solute with a neighboring molecule. Studies of the lowest-energy conformation have been applied to the configuration of benzene dimers in water [24–26].

The object of this work was to elucidate the properties of the fluorinated phase with respect to the structure–retention relationship using hydrocarbons as the solute and making a comparison with the hydrocarbonaceous phase, and to explain the retention mechanism by introducing a computer simulation method.

2. Experimental

A branched fluorocarbonaceous bonded silica gel (Fluofix, Neos, Kobe, Japan), a linear fluorocarbonaceous bonded silica gel (F-L6, Neos, not commercially available) and a conventional octyl-bonded silica gel (Neos C_8) were used. To prevent effects on the retention behavior due to the nature of the surface structure of the base silica gels, all of the packing materials were prepared starting from the same batch of high-purity silica gel. Silylation of Fluofix was carried out with a 1*H*,1*H*,2*H*,2*H*,3*H*,3*H*-tridecafluoro(4,4-dimethylheptyl)dimethyl agent [27]. F-L6 was prepared by silylation with 1*H*,1*H*,2*H*,2*H*-perfluorooctyl dimethyl agents. Two hydrocarbonaceous columns, a Nucleosil C_{18} (Macherey Nagel) and a Neos C_8, were used as reference. The physico-chemical characteristics of the packing materials are given in Table 1. These gels were

Table 1
Physico-chemical characteristics of the chemically bonded phase

	Fluofix [28] branched type	F6 [28] linear type	Neos C_8 [28]	Nucleosil C_{18} [29]
Mean particle size (μm)	5	5	5	5
Particle shape	Spherical	Spherical	Spherical	Spherical
End capped	Yes	Yes	Yes	Yes
Specific surface area (m^2/g)	343	343	343	300
Carbon content (%)	8.48	8.42	9.79	15–16
Coverage ($\mu mol/m^2$)	2.49	2.69	2.56	–
($groups/nm^2$)	1.57	1.62	1.61	–
Pore size	120	120	120	100

packed into stainless steel tubes (15 or 25 cm long, 4.6 mm I.D.).

The chromatographic system consisted of a Shimadzu Model LC-10A chromatograph, a Model CTO-2A column oven, a Model SPD-M10A UV detector, (Shimadzu, Kyoto, Japan) and a Model RI-SE51 refractometer (Showa Denko, Tokyo, Japan). A Model 7125 sample injector (Rheodyne, CA, USA) was installed in the column oven to prevent a temperature gradient along the column.

Chromatography was carried out with methanol–water eluents with a mixing ratio ranging from 50:50 to 90:10 (v/v). The eluate was monitored with a UV detector for aromatic hydrocarbons and with a refractometer for *n*-alkanes. All measurements of retention were made in triplicate. The value of the retention factor, *k*, was determined by the usual method: $k = (t_R - t_0)/t_0$, where t_R is the solute retention time and t_0 the column hold up time. In this work, the retention time of sodium nitrite was taken as the column hold up time. The deviation of $\ln k$ from the average of the triplicate measurements for each compound was within 0.3%.

Calculation of the solvent accessible surface (SAS) area and the nonbonding molecular interaction energy was carried out on a CAChe system (Sony Tectronix, Tokyo, Japan) using a CAChe MOPAC with PM3 parameters for the geometrically optimized solute molecule and a linear fluorinated ligand. The effects of solvation by solvent molecules were estimated by applying two methods, the COSM method and a search for the lowest-energy conformation.

Aromatic hydrocarbons, and other chemicals of analytical reagent grade, were purchased from Nacalai Tesque (Kyoto, Japan).

3. Results and discussion

Twenty-one hydrocarbons were chromatographed on the Fluofix column or on the Neos C_8 column with an 80:20 (v/v) methanol–water mixed eluent at 50°C. For the comparison of the retention properties of the fluorinated and hydrocarbonaceous phases, logarithms of the retention factors measured on the Fluofix column, $\ln k_F$, were plotted against the corresponding values on the Neos C_8 column, $\ln k_C$ (Fig. 1). Five linear lines with slopes less than unity

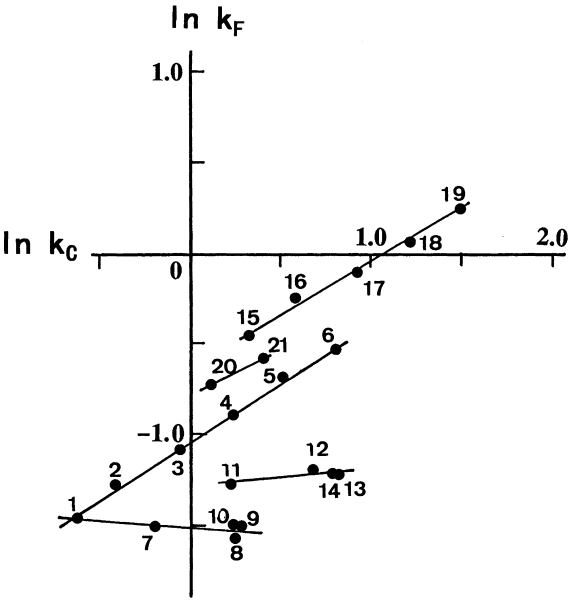

Fig. 1. Correlation plots of the logarithm of the retention factor on the Fluofix column, $\ln k_F$, versus the value on the C_8 column, $\ln k_C$. Eluent, methanol–water, 80:20 (v/v); temperature, 50°C. Solutes: (1) benzene, (2) toluene, (3) ethylbenzene, (4) *n*-propylbenzene, (5) *n*-butylbenzene, (6) *n*-amylbenzene, (7) naphthalene, (8) phenanthrene, (9) anthracene, (10) fluorene, (11) diphenylmethane, (12) *o*-terphenyl, (13) *m*-terphenyl, (14) *p*-terphenyl, (15) *n*-pentane, (16) *n*-hexane, (17) *n*-heptane, (18) *n*-octane, (19) *n*-nonane, (20) cyclopentane, (21) cyclohexane.

were constructed for five homologous families: *n*-alkanes, cycloparaffins, *n*-alkylbenzes, polyaromatics and condensed aromatics. The values of the slopes for the five homologous groups are listed in Table 2. The slope of the correlation curves for the columns represents the ratio of the Gibbs' free energy changes for the transfer of the solute from the stationary

Table 2
Comparison of the slopes of the correlation curves for the Fluofix column and the Neos C_8 column

Homologous group	Number of plots in Fig. 2	Slope
n-Alkanes	15–19	0.57
Cycloparaffins	20, 21	0.48
n-Alkylbenzenes	2–6	0.61
Polyaromatic hydrocarbons	11–14	0.10
Benzene	1	
Condensed aromatic hydrocarbons	7–10	−0.07

phase to the mobile phase [30]. For example, the Gibbs' retention energy of *n*-alkanes on the Fluofix column was smaller than that on the C_8 column by 0.57 times. Similarly, the retention energy of polyaromatics on the Fluofix column was one-tenth that on the C_8 column. The gentle slope for the polyaromatics indicates a lower selectivity on the Fluofix column than on the C_8 column. For the correlation curve of the condensed aromatics, a slightly negative slope was obtained. A negative slope implies that the elution order of the condensed aromatics on the Fluofix column was the reverse of that on the Neos C_8 column.

The effects of the methanol concentration on selectivity for condensed aromatics, such as benzene, naphthalene, fluorene, phenanthrene and anthracene, were studied on the Fluofix column with various proportions of methanol–water mixed solvent ranging from 50:50 to 90:10 (v/v). Using the solvent accessible surface (SAS) area as the parameter for the solute molecular size, a linear curve was obtained on a plot of ln *k* versus SAS area. The slope, $\Delta \ln k$/SAS area, represents the selectivity normalized by the molecular size. Fig. 2 shows a plot of $\Delta \ln k$/SAS area versus the concentration of methanol. $\Delta \ln k$/SAS on the Nucleosil C_{18} column decreased with increasing concentration of methanol in the eluent and converged to a positive value near zero, as shown in curve A of Fig. 2. The elution order of the solutes was independent of the methanol concentration. $\Delta \ln k$/SAS on the Fluofix column decreased to a negative value with increasing concentration of methanol, as shown in curve B of Fig. 2. The aromatics were eluted in the order of molecular size within the positive range of $\Delta \ln k$/SAS. Within the negative range the elution order was inverted and the larger aromatic solute was less retained.

A typical chromatogram of benzene and anthracene on the Fluofix column with 90:10 (v/v) methanol–water is shown in Fig. 3. The benzene peak was found to elute after that of anthracene. The effects of the organic modifier concentration on the retention of the condensed aromatics suggests the existence of size exclusive interactions at higher methanol concentration on the Fluofix column.

The column temperature often plays an important role in the retention behavior of solutes. In this work, retention of the solute was accelerated at higher temperature. However, the elution order of the solutes in the homologous group was independent of the temperature in the range 35 to 60°C.

In order to confirm the effect of methanol concentration on the relationship between retention and the molecular size of the aromatics, 21 polycyclic aromatic hydrocarbons were chromatographed using two different concentrations of methanol–water eluent and the Fluofix column (4.6×250 mm). The polycyclic aromatic hydrocarbons examined and

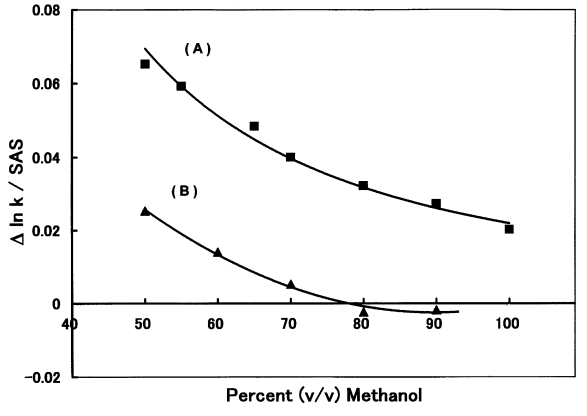

Fig. 2. Plots of $\Delta \ln k$/SAS area for the aromatics versus the concentration of methanol in the eluent. (A) 4.6×150 mm Nucleosil C_{18} column. (B) 4.6×150 mm Fluofix column. Temperature, 60°C. Solutes: benzene, naphthalene, fluorene, phenanthrene, anthracene.

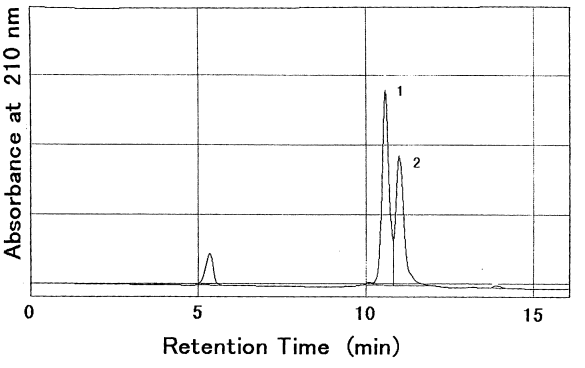

Fig. 3. Chromatogram of anthracene and benzene. Column, 4.6×250 mm Fluofix; temperature, 50°C; flow-rate, 0.3 ml/min; eluent, methanol–water, 90:10 (v/v). Solutes: (1) anthracene, (2) benzene.

Table 3
Polycyclic aromatic hydrocarbons and their solvent accessible surface area

	Benzene and PAH solutes	SAS area[a]
1	Benzene	59.00
2	Naphthalene	77.98
3	Fluorene	92.20
4	Phenanthrene	95.83
5	Anthracene	96.62
6	Pyrene	100.63
7	Fluoranthene	103.82
8	Crysene	113.55
9	Naphthacene	115.13
10	Coronene	126.84
11	Pentacene	134.51
12	Diphenyl	90.75
13	Diphenylmethane	98.14
14	*o*-Terphenyl	118.57
15	*m*-Terphenyl	122.51
16	*p*-Terphenyl	122.61
17	β-Methoxynaphthalene	88.79
18	1-Methylnapthalene	83.37
19	2,3-Dimethylnaphthalene	90.10
20	Dihydropyrene	100.97
21	9,10-Dimethyl-1,2-benzanthracene	125.66

[a] Calculated using the CAChe system.

their SAS areas calculated using the CAChe system are listed in Table 3.

For elution with 50:50 (v/v) methanol–water mixed solvent at 50°C, the ln k values of aromatic compounds versus the SAS area are plotted in Fig. 4. The number given for each plot in Fig. 4 corresponds to that of the compounds in Table 3. The retention of the aromatic compounds increased with the SAS area. A correlation curve with a positive slope is drawn through the plots of the planar and narrow shaped aromatic solutes, such as benzene, naphthalene, anthracene, naphthacene and pentacene (points 1, 2, 5, 9 and 11, respectively, in Fig. 4). Most of the plots, except for the methyl and methoxy derivatives of naphthalene, fall on a linear correlation curve. The plots for naphthalene, 1-methylnaphthalene and 2,3-dimethyl-naphthalene (points 2, 18 and 19, respectively, in Fig. 4) are shown on the branched dotted line with a positive and steeper slope than that for the unsubstituted solutes. A substituted methyl group enhances the molecular interaction between the solute and the ligand. On the other hand, the retention of β-methoxynaphthalene (point 17 in Fig. 4), having a hydrophilic group, is

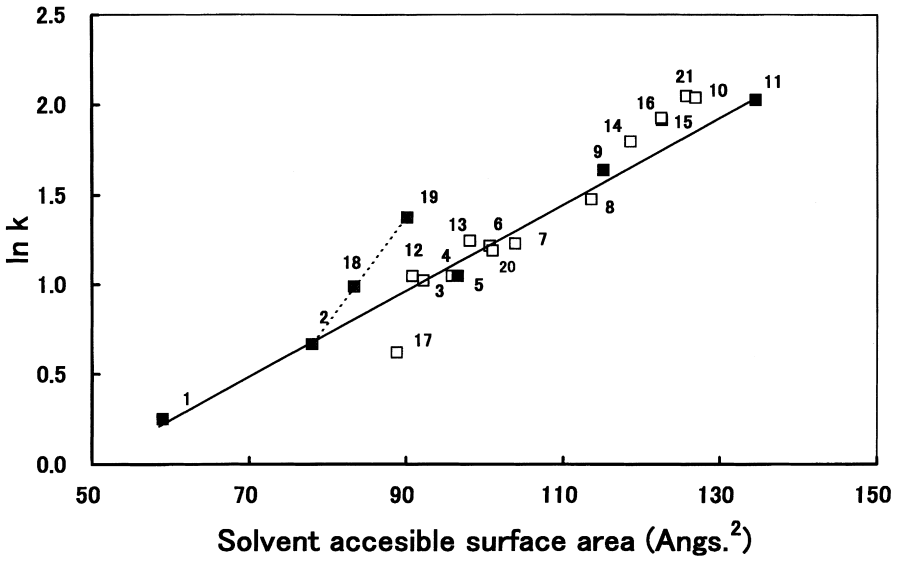

Fig. 4. Correlation plots of ln k versus SAS area of the solute molecule. Column, 4.6×250 mm Fluofix; temperature, 50°C; flow-rate, 0.3 ml/min; eluent, 50:50 (v/v) methanol–water mixed solvent. Solutes: (1) benzene, (2) naphthalene, (3) fluorene, (4) phenanthrene, (5) anthracene, (6) pyrene, (7) fluoranthene, (8) crysene, (9) naphthacene, (10) coronene, (11) pentacene, (12) diphenyl, (13) diphenylmethane, (14) *o*-terphenyl, (15) *m*-terphenyl, (16) *p*-terphenyl, (17) β-methoxynaphthalene, (18) 1-methyl naphthalene, (19) 2,3-dimethylnaphthalene, (20) di-hydropyrene, (21) 9,10-dimethyl 1,1,2-benzanthracene.

suppressed and elutes before naphthalene, although the SAS area of β-methoxynaphthalene is larger than that of naphthalene.

A drastic change in the elution order with methanol concentration is seen in Fig. 5. The ln *k* values are plotted against the SAS area of the solute for elution with 90:10 (v/v) methanol–water solution. A correlation curve with negative slope is drawn through the plots of the planar and narrow shaped aromatic solutes, such as benzene, naphthalene, anthracene, naphthacene and pentacene (points 1, 2, 5, 9 and 11, respectively, in Fig. 5). The plots of the other planar aromatic solutes, such as fluorene, phenanthrene, pyrene, fluorancene, chrysene and coronene (points 3, 4, 6, 7, 8, and 10, respectively, in Fig. 5), fall on the linear correlation curve. Plots for the nonplanar and nonrigid aromatic groups including diphenyl, *o*-, *m*- and *p*-terphenyls, diphenylmethane and 9,10-dimethyl-1,2-benzanthracene (points 12, 14, 15, 16, 13, and 21, respectively, in Fig. 5) deviate above the line through the plots of the narrow solutes. The retention of naphthalene derivatives increases with the number of substituted methyl groups, whereas it decreases with the introduction of the methoxy group. Dihydropyrene (point 20 in Fig. 5), having one less aromatic ring than pyrene (point 6 in Fig. 5), was retained more than pyrene.

Table 4
Values of β (K) for the retention of aromatics

MeOH (%)	Column		
	Fluofix	Neos C_8	Nucleosil C_{18}
50	484	–	609
60	451	–	624
70	368	–	603
80	294	519	593

The existence of exclusive interactions between the aromatic molecule and the fluorinated phase is confirmed from Fig. 5. The exclusive molecular interactions were stronger for the retention of the planar and rigid solutes than for the nonplanar solutes and increased with the number of aromatic rings. Figs. 4 and 5 demonstrate the dependence of the retention mechanism on the methanol concentration in the eluent.

Table 4 shows values of the enthalpy–entropy compensation temperature, β, for the retention of condensed aromatic hydrocarbons on the Fluofix,

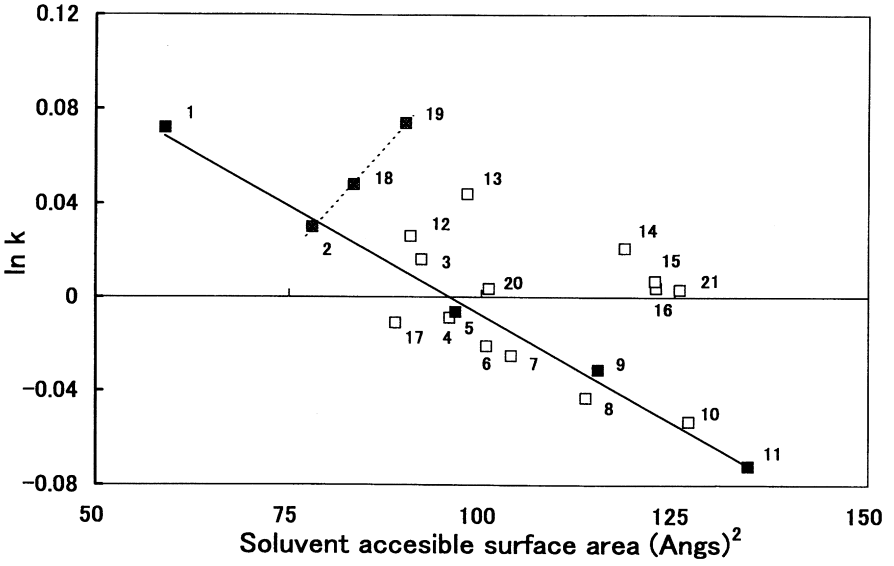

Fig. 5. Correlation plots of ln *k* and SAS area for the solutes. Eluent, 90:10 (v/v) methanol–water mixed solvent. Other experimental conditions are the same as in Fig. 4.

Nucleosil C_{18} and Neos C_8 columns. The β values for the Nucleosil C_{18} column were 600 K or thereabouts with methanol–water mixed eluent in the range from 50:50 to 80:20 (v/v). No effect of the methanol concentration in the eluent on the β values was observed. The β value on the C_8 column was 519 K in 80:20 (v/v) methanol–water mixed eluent. The β values on the two hydrocarbonaceous columns were identified from the reported values in reversed-phase chromatography governed by hydrophobic interactions [31,32]. On the contrary, the β value on the Fluofix column was 484 K at a methanol concentration of 50:50 (v/v), and decreased noticeably with increasing methanol concentration. The concentration dependence of the β value also indicates that the retention mechanism of aromatics on the Fluofix column is controlled by the concentration of methanol in the eluent.

The solute–stationary phase interaction was investigated by calculating the potential energy for the formation of the complex [solute–ligand] by computer simulation. Prior to the calculation, two fluorinated columns, Fluofix with a branched bonded ligand and F-L6 with a linear bonded ligand, were applied to compare the effects of the ligand structure on the retention properties.

Five homologous families of hydrocarbons were eluted with four different concentrations of methanol–water mixed solvent in the range 50:50 to 80:20 (v/v). Fig. 6 shows the value of $\ln k_F$ plotted against those on the F-L6 column, $\ln k_{F\text{-}L6}$. A linear correlation curve with a correlation coefficient of 0.999 was obtained for all plots. The slope of 0.98 for the correlation curve indicates that the selectivity of the hydrocarbons on the Fluofix column is consistent with that on the F-L6 column. A linear ligand was applied to the computer simulation of the molecular interaction for simplicity of the [solute–ligand] model.

Considering the intermolecular interaction between the solute and surrounding solvent molecules in addition to the solute–ligand interaction, the

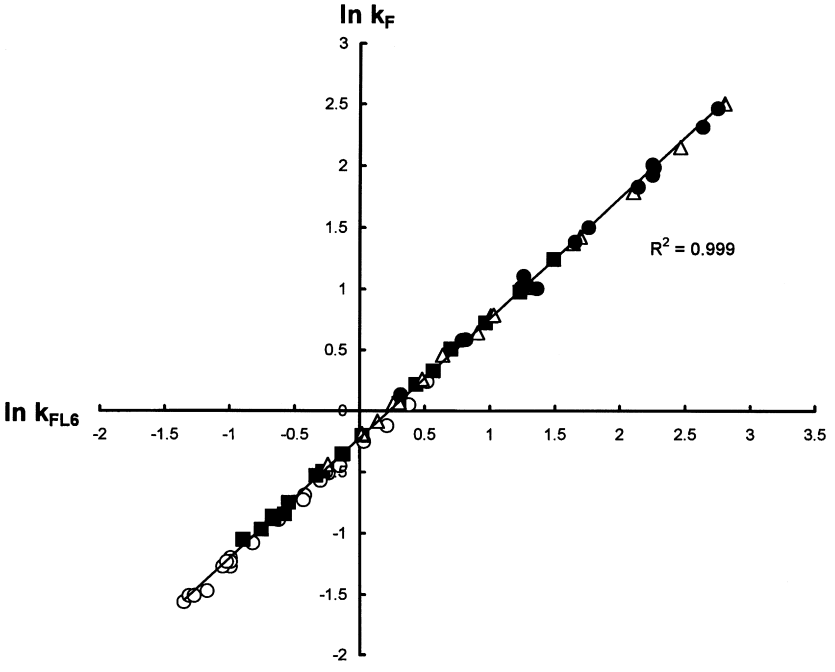

Fig. 6. Correlation plots of the logarithm of the retention factor on the Fluofix column, $\ln k_F$, versus the value on the F-L6 column, $\ln k_{F\text{-}L6}$. Eluent: (●) methanol–water, 50:50 (v/v); (△) 60:40 (v/v); (■) 70:30 (v/v); (○) 80:20 (v/v). Temperature, 50°C. Solutes are the same as in Fig. 1. The number on the plots is not given.

calculation was carried out first using the COSMO method. Two extreme attitudes of the aromatic molecules to the ligand were applied for formation of the complex. In one attitude the plane of the aromatic ring faced the ligand (P type). In the other attitude the edge of the aromatic ring faced the ligand (V type).

Fig. 7 shows the potential energy curves for the formation of the P and V types of naphthalene–fluorocarbon ligand in 50:50 and 90:10 (v/v) methanol–water mixed solvents, respectively. The minimum structure for the naphthalene–fluorocarbon ligand was obtained in P-type complex formation at a carbon–carbon intermolecular distance, R_{C-C}, of 6.6 Å between the naphthalene and ligand molecules in both 50:50 and 90:10 (v/v) methanol–water mixed solvents. The energy curve for the complex in the V type structure increased with decreasing R_{C-C}. The minimum structure was not observed in V-type complex formation. Similarly, for the formation of benzene–fluorocarbon ligand and of anthracene–fluorocarbon ligand, the minimum structure was obtained in the P-type formation. The potential energy curve suggests that the aromatic molecule forms a complex with the fluorocarbon ligand preferentially in the attitude of the P-type structure.

Fig. 8 shows the case of complex formation of a naphthalene molecule with a C_8 ligand. The minimum structure of the naphthalene–C_8 ligand was not found in the P-type but in the V-type structure at $R_{C-C} = 3.8$ Å. The naphthalene molecule prefers to form a complex with the C_8 ligand in the V-type structure, unlike the complex with the fluorocarbon ligand.

Values of the potential energy for complex formation of the aromatics with fluorocarbon ligand or C_8 ligand are presented in Table 5. The potential energy for complex formation of the condensed aromatics–fluorocarbon ligand was about one-twentieth that of the aromatics–C_8 ligand. The minimum R_{C-C} for the aromatics–fluorocarbon ligand complex was larger than that for the aromatics–C_8 ligand complex. The aromatic solute molecule cannot approach as close to the fluorinated ligand as to the C_8 ligand. The smaller retention of aromatics on the Fluofix column can be explained from a comparison of the potential energy for complex formation.

The preference for the P-type structure for the

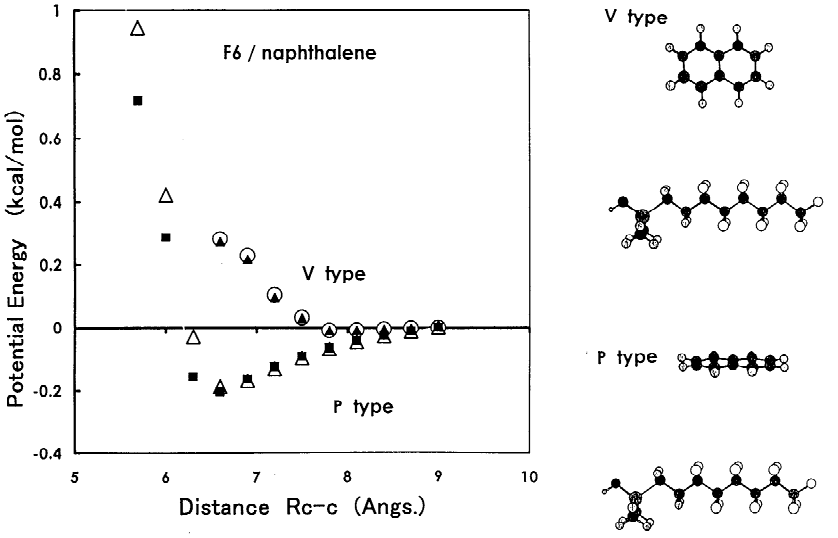

Fig. 7. Potential energy curves for the formation of the complex of naphthalene and fluorinated ligand. (△) The plane of the naphthalene molecule approaches the fluorinated ligand in 50:50 (v/v) methanol–water mixed solvent. (■) The plane of the naphthalene molecule approaches the fluorinated ligand in 90:10 (v/v) methanol–water mixed solvent. (○) The edge of the ring of the naphthalene molecule approaches the fluorinated ligand in 50:50 (v/v) methanol–water mixed solvent. (▲) The edge of the ring of the naphthalene molecule approaches the fluorinated ligand in 90:10 (v/v) methanol–water mixed solvent.

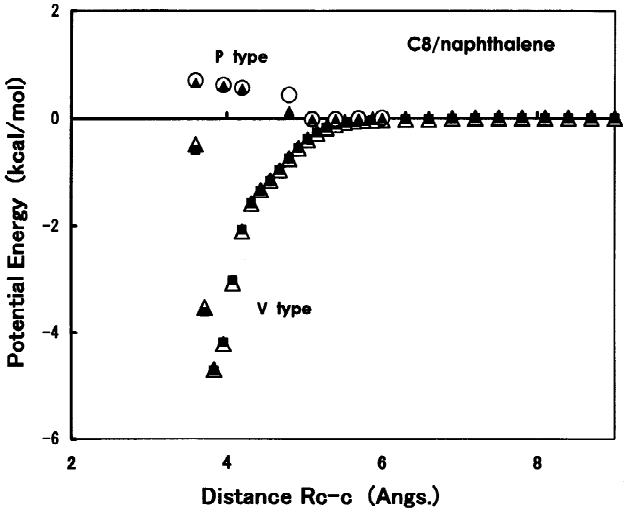

Fig. 8. Potential energy curves for the formation of a complex between naphthalene and C_8 ligand. (△) The plane of the naphthalene molecule approaches the C_8 ligand in 50:50 (v/v) methanol–water mixed solvent. (■) The plane of the naphthalene molecule approaches the C_8 ligand in 90:10 (v/v) methanol–water mixed solvent. (○) The edge of the ring of the naphthalene molecule approaches the C_8 ligand in 50:50 (v/v) methanol–water mixed solvent. (▲) The edge of the ring of the naphthalene molecule approaches the C_8 ligand in 90:10 (v/v) methanol–water mixed solvent.

attitude of the aromatic compound with respect to the fluorinated ligand suggests the existence of electrostatic interactions between the π-electron on the aromatic rings and the electron-donor fluorine atom in the fluorocarbon group, having a lone pair of electrons on the 2p orbital. The interactions increase with the number of π-electrons on the aromatic rings, as shown in Table 5.

No effect of the concentration of methanol in the solvent on the potential energy was observed in the simulation using the COSMO method, as shown in Fig. 7. In the next step, considering the orientation of the methanol molecules close to the solute molecule in the methanol aqueous solvent, the nonbonding molecular interaction energy of the methanol–solute was calculated. Fig. 9 shows the potential energy curves computed for three extreme conformations of the benzene–methanol complex. In the type A potential energy curve of Fig. 9 the methyl residue of the methanol molecule approaches along the benzene symmetry axis perpendicularly. As the calculated potential energy of the type A complex was nearly zero, it is hard for a methanol molecule to approach along the benzene symmetry axis perpendicularly. In the type B complex the methyl residue of the methanol molecule approaches the carbon atom of the benzene ring perpendicularly and is tilted away from the benzene symmetry axis. The potential energy in this type was 0.37 kcal/mol. The most preferential orientation was the type C complex with a potential energy of 0.64 kcal/mol, where the methyl residue of the methanol molecule approaches the benzene plane horizontally. In a low methanol concentration, the benzene molecule is assumed to be preferentially solvated with methanol molecules in the type C orientation. With an increase in the

Table 5
Potential energy for complex formation of the aromatics with ligand[a]

Solute–ligand	Benzene	Naphthalene	Anthracene
Aromatic–fluorinated ligand	0.19	0.27	0.32
Aromatic–C_{18} ligand	3.9	4.6	6.2

[a] The average potential energy (kcal/mol) obtained in the range 50:50 to 90:10 (v/v) methanol–water mixed solvent.

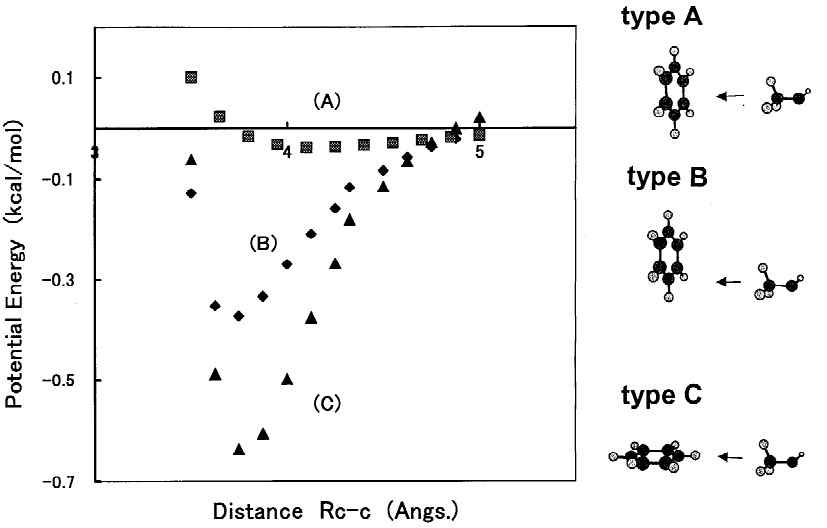

Fig. 9. Potential energy curves for the formation of the benzene–methanol complex. Type A: the methanol molecule approaches perpendicular to the plane of the ring of the benzene molecule. The methyl residue of methanol approaches along the benzene symmetry axis. Type B: the methanol molecule approaches perpendicular to the plane of the ring of the benzene molecule. The methyl residue of methanol approaches the carbon atom of the benzene ring. Type C: the methanol molecule approaches in the benzene plane.

concentration of methanol, the population of the benzene–methanol quasi-molecule in type B orientation might be increased.

The potential energy of complex formation for the fluorinated ligand–methanol was 0.02 kcal/mol, which is sufficiently low to neglect the solvation of the fluorinated ligand with methanol molecules. On the other hand, the potential energy of complex formation for the aromatics–methanol molecule was comparable to that of the aromatics–fluorinated ligand. Formation of the ternary complex of the benzene–methanol quasi-molecule and the fluorinated ligand was postulated. At lower methanol concentrations, the benzene–methanol quasi-molecule in the dominant type C configuration approaches the fluorinated ligand to form a ternary complex in the P type attitude, as illustrated in Fig. 10 (type I). With increasing methanol concentration the benzene–methanol quasi-molecule in the type B orientation approaches the fluorinated ligand to form a ternary complex, as illustrated in Fig. 10 (type II). The solvating methanol molecule may increase the distance between benzene and the ligand and block the formation of the benzene–ligand complex to reduce the intermolecular interaction between the solute and stationary phase. Consequently, the retention of benzene is weakened with increasing methanol concentration in the eluent. In the case of the retention of fused-ring aromatic compounds, the number of perpendicularly oriented methanol molecules increases with the number of aromatic rings, and, subsequently, the effect of steric obstruction by the methanol molecules increases the retention of aromatics with solute size and the methanol con-

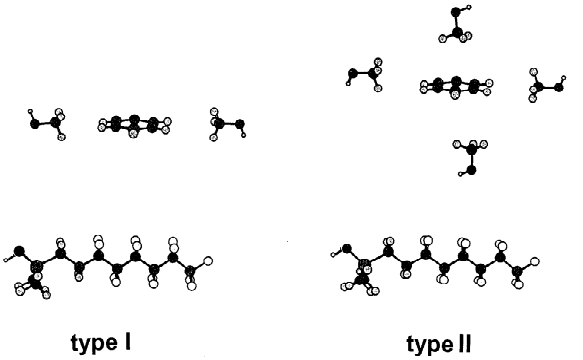

Fig. 10. Schematic representation of the attitude of the benzene molecule to the fluorinated ligand. Type I: when the concentration of methanol is low, methanol molecules are oriented horizontally with respect to the benzene ring. Type II: when the concentration of methanol is high, the methanol molecules are oriented perpendicularly with respect to the benzene ring.

centration in the eluent. And, with the attitude in the P type complex, the retention of planar aromatics is likely to be obstructed by methanol molecules in comparison with nonplanner aromatics.

The concentration dependence shown in Fig. 5 was elucidated by simulation of the attitude of the aromatics with respect to the stationary ligand and a neighboring methanol molecule. Two increasing competitive interactions with the solute molecular size, the electrostatic interaction between the π-electron and a fluorine atom, and steric obstruction by the solvent molecule, were observed between the solute and the fluorinated ligand. With increasing concentration of methanol in the eluent, the retention of the solute due to electrostatic molecular interactions decreased, and the exclusive interaction became dominant in the retention of the aromatic solutes.

In the case of complex formation with the C_8 ligand, the potential energy for the formation of benzene–C_8 ligand was 3.9 kcal/mol, as shown in Table 5. This value is significantly larger than that for benzene–methanol quasi-molecules in type B or C orientation. When the benzene–methanol quasi-molecule accesses the C_8 ligand, a weakly bonded methanol molecule is released to establish a new binary benzene–C_8 ligand complex. The retention mechanism of the aromatics on the C_8 ligand was not affected by the concentration of methanol in the eluent.

Computer simulation was a useful nonchromatographic tool for the elucidation of the retention mechanism. Important information was obtained by considering the attitude of the solute molecule with respect to the ligand of the stationary phase and the neighboring methanol molecule.

Acknowledgements

The authors thank Dr. F. Nemoto at Neos for preparing the fluorinated columns.

References

[1] P.J. Schoenmakers, H.A.H. Billet, L. de Galan, Chromatographia 15 (1982) 205.
[2] W.H. Pirkle, D.W. House, J.M. Finn, J. Chromatogr. 192 (1980) 143.
[3] X. Geng, P.W. Carr, J. Chromatogr. 269 (1983) 96.
[4] G.E. Berenndesen, K.A. Pikaart, L. de Galan, Anal. Chem. 52 (1980) 1990.
[5] P.C. Sadek, P.W. Carr, J. Chromatogr. 288 (1984) 25.
[6] H.A.H. Billet, P.J. Schoenmakers, L. de Galan, J. Chromatogr. 218 (1981) 443.
[7] C. Hirayama, H. Ihara, S. Nagaoka, K. Hamada, J. Chromatogr. 65 (1989) 241.
[8] T. Yuno, T. Monde, T. Kamiusuki, K. Mikumo, H. Kohama, T. Konakahara, in: Proceedings of the 3rd International Conference on High Technology, Chiba, Japan, 1992.
[9] S.A. Wise, W.J. Bonner, F.R. Guenther, W.E. May, J. Chromatogr. Sci. 19 (1981) 457.
[10] L.C. Sander, S.A. Wise, Anal. Chem. 67 (1995) 3284.
[11] M. Pursch, L.C. sander, K. Albert, Anal. Chem. 68 (1996) 4107.
[12] M. Pursch, L.C. Sander, H.J. Egelhaaf, M. Ritza, A. Wise, D. Oelkrug, K. Albert, J. Am. Chem. Soc. 121 (1999) 3210.
[13] K. Jinno, T. Nagoshi, N. Tanaka, M. Okamoto, J.C. Fetzer, W.R. Biggs, J. Chromatogr. 386 (1987) 123.
[14] B. Buszewski, M. Jezierska, M. Welniak, R. Kaliszan, J. Chromatogr. A 845 (1999) 433.
[15] T. Shindo, Y. Shimabukuro, T. Kanamori, T. Iwatsubo, Y. Nagawa, K. Hiratani, J. Chromatogr. A 877 (2000) 61.
[16] Q.H. Wan, L. Ramaley, R. Guy, Chromatographia 46 (1997) 495.
[17] H. Carlsson, C. Ostmann, J. Chromatogr. A 715 (1995) 31.
[18] R. Rosset, Analysis 15 (1987) 1.
[19] L.C. Sander, S.A. Wise, Anal. Chem. 59 (1987) 2309.
[20] K.A. Dill, J. Phys. Chem. 91 (1987) 1980.
[21] I. Yarovsky, M.-I. Aguilar, M.T.W. Hearn, Anal. Chem. 67 (1995) 2145.
[22] G.L. Heard, R.J. Boyd, J. Phys. Chem. A 101 (1997) 5374.
[23] A. Klamt, G. Schuurmann, J. Chem. Soc., Perkin Trans. 2 (1993) 799.
[24] P. Linse, G. Karlström, B. Jönsson, J. Am. Chem. Soc. 106 (1984) 4096.
[25] G. Ravishanker, P.K. Mehrotra, D.L. Beveridge, J. Am. Chem. Soc. 106 (1984) 4102.
[26] P. Linse, J. Am. Chem. Soc. 114 (1992) 4366.
[27] T. Kamiusuki, T. Monde, K. Yano, T. Yoko, T. Konakahara, Chromatographia 49 (1999) 649.
[28] T. Monde, private communication.
[29] R.E. Majors, J. Chromatogr. Sci. 18 (1980) 488.
[30] W. Melander, J. Stoveken, Cs. Horvath, J. Chromatogr. 199 (1980) 35.
[31] W. Melander, D.E. Campbell, Cs. Horvath, J. Chromatogr. 158 (1978) 215.
[32] J.H. Knox, G. Vasvary, J. Chromatogr. 83 (1973) 181.